International Journal of Fluid Machinery and Systems
Vol. 4, No. 1, January-March 2011

DOI: 10.5293/IJFMS.2011.4.1.179
ISSN (Online): 1882-9554

Original Paper (Invited)

Experimental Investigations on Upper Part Load Vortex Rope Pressure Fluctuations in Francis Turbine Draft Tube

Christophe Nicolet[1], Amirreza Zobeiri[2], Pierre Maruzewski[2] and François Avellan[2]

[1]Power Vision Engineering sàrl, 1 ch. des Champs-Courbes, CH-1024 Ecublens, Switzerland
christophe.nicolet@powervision-eng.ch
[2] Laboratory for Hydraulic Machines, Ecole Polytechnique Fédérale de Lausanne, EPFL,
CH-1015 Lausanne, Switzerland
amirreza.zobeiri@epfl.ch, pierre.maruzewski@epfl.ch, francois.avellan@epfl.ch

Abstract

The swirling flow developing in Francis turbine draft tube under part load operation leads to pressure fluctuations usually in the range of 0.2 to 0.4 times the runner rotational frequency resulting from the so-called vortex breakdown. For low cavitation number, the flow features a cavitation vortex rope animated with precession motion. Under given conditions, these pressure fluctuations may lead to undesirable pressure fluctuations in the entire hydraulic system and also produce active power oscillations. For the upper part load range, between 0.7 and 0.85 times the best efficiency discharge, pressure fluctuations may appear in a higher frequency range of 2 to 4 times the runner rotational speed and feature modulations with vortex rope precession. It has been pointed out that for this particular operating point, the vortex rope features elliptical cross section and is animated of a self-rotation. This paper presents an experimental investigation focusing on this peculiar phenomenon, defined as the upper part load vortex rope. The experimental investigation is carried out on a high specific speed Francis turbine scale model installed on a test rig of the EPFL Laboratory for Hydraulic Machines. The selected operating point corresponds to a discharge of 0.83 times the best efficiency discharge. Observations of the cavitation vortex carried out with high speed camera have been recorded and synchronized with pressure fluctuations measurements at the draft tube cone. First, the vortex rope self rotation frequency is evidenced and the related frequency is deduced. Then, the influence of the sigma cavitation number on vortex rope shape and pressure fluctuations is presented. The waterfall diagram of the pressure fluctuations evidences resonance effects with the hydraulic circuit. The influence of outlet bubble cavitation and air injection is also investigated for low cavitation number. The time evolution of the vortex rope volume is compared with pressure fluctuations time evolution using image processing. Finally, the influence of the Froude number on the vortex rope shape and the associated pressure fluctuations is analyzed by varying the rotational speed.

Keywords: Francis turbine, cavitating vortex rope, High Speed Camera visualization, pressure fluctuations.

1. Introduction

The vortex rope precession frequency commonly corresponds to 0.2 to 0.4 times the turbine rotational frequency *n*, and may also induce pressure fluctuations in a higher frequency range between 2·n to 4·n, for high specific speed turbines at upper part load range as described by Fisher in 1980 [1], Dörfler in 1994 [2] and Jacob in 1996 [3]. Figure 1 presents a waterfall diagram of pressure fluctuations measured in the draft tube cone of a Francis turbine showing both part load pressure fluctuations and upper part load pressure fluctuations. Moreover, a ”shock phenomenon” may occur in the same operating range and induce structural vibrations due to vortex rope impacts on the draft tube wall as illustrated in

Fig. **2** left, [2]. This shock phenomenon provides energy on a wide frequency range as illustrated in

Fig. **2** right, [4], [5]. Upper part load pressure fluctuations may also leads to resonance between harmonics of the vortex rope and the test rig, [4]. In case of resonance, the pressure fluctuations in the range 2·n to 4·n can be found in the whole draft tube and at the spiral case inlet while the pressure fluctuations related to the vortex rope precession are restricted to the vicinity of the draft tube cone, see Fig. 3. Koutnik *et al.* [6] performed investigations for different rotational speeds but for the same operating point, *i.e.* assessing the Froude influence, and pointing out that the pressure fluctuations can occur even if the predominant amplitudes

Accepted for publication February 11 2011: Paper number O11004S
Corresponding author: Christophe Nicolet, Managing co-director, christophe.nicolet@powervision-eng.ch
This manuscript was presented at the 25th IAHR Symposium on Hydraulic Machinery and Systems, September 20-24, 2010, Politechnica University of Timisoara, Romania .

are not found at a frequency being a multiple of the vortex rope precession. Therefore, the origin of these pressure fluctuations can not only be induced by the shock phenomenon. In addition, the physical modulation process was identified by Koutnik *et al.* [6] to be related to the elliptical shape of the vortex rope cross section observed on test rig at upper part load. The motion of the elliptical vortex rope at upper part load can be decomposed in precession movement with pulsation ω_{rope} and the self rotation of the vortex rope with pulsation ω_{sr} as it is illustrated in Fig. 4. Haban *et al.* [7] demonstrated that the elliptical shape of the vortex rope can be predicted by modal analysis of a simplified draft tube flow. Koutnik *et al.* [8] analyzed the influence of air injection and hydraulic circuit on the upper part load pressure fluctuations. The elliptical shape of the vortex rope was also investigated using PIV measurements by Kirschner *et al.* [9] on a simplified draft tube.

This paper is a contribution to the analysis of the upper part load pressure fluctuations by means of high speed camera visualization with synchronized measurement of pressure fluctuations. First, the test case and related experimental apparatus is described. Then, image post processing is used to derive vortex rope diameter time evolution and to compare with to synchronized pressure fluctuations. The influence of both sigma cavitation number and Froude number are analyzed to show the interaction between the upper part load fluctuations and the hydraulic circuit. The influence of outlet bubble cavitation and air injection is also investigated.

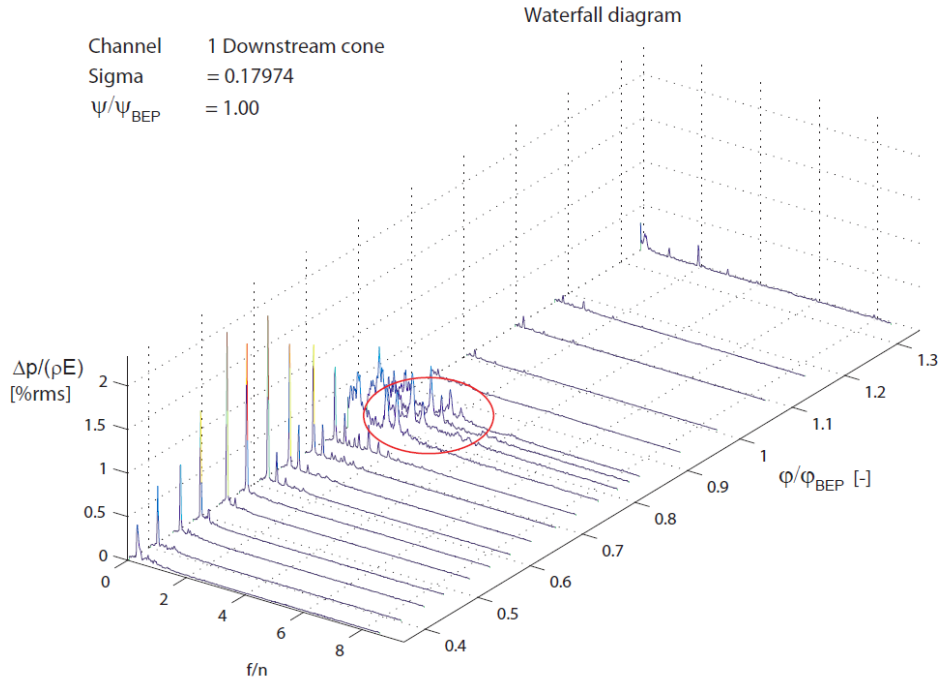

Fig. 1 Waterfall diagram of the pressure fluctuations measured at the downstream cone of the draft tube

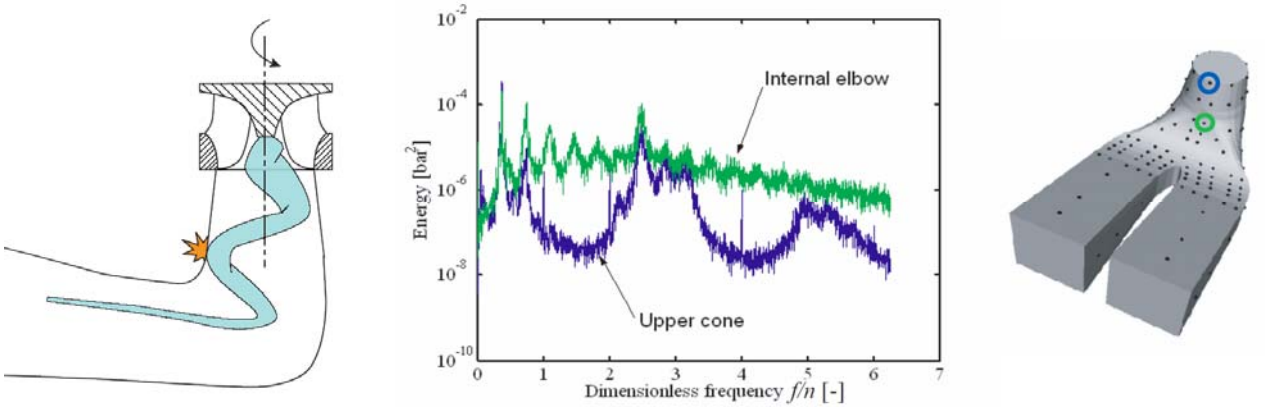

Fig. 2 Schematic representation of the "Shock phenomenon" (left) and the resulting pressure energy spectra in the inner part of the draft tube elbow (center and right), see [4]

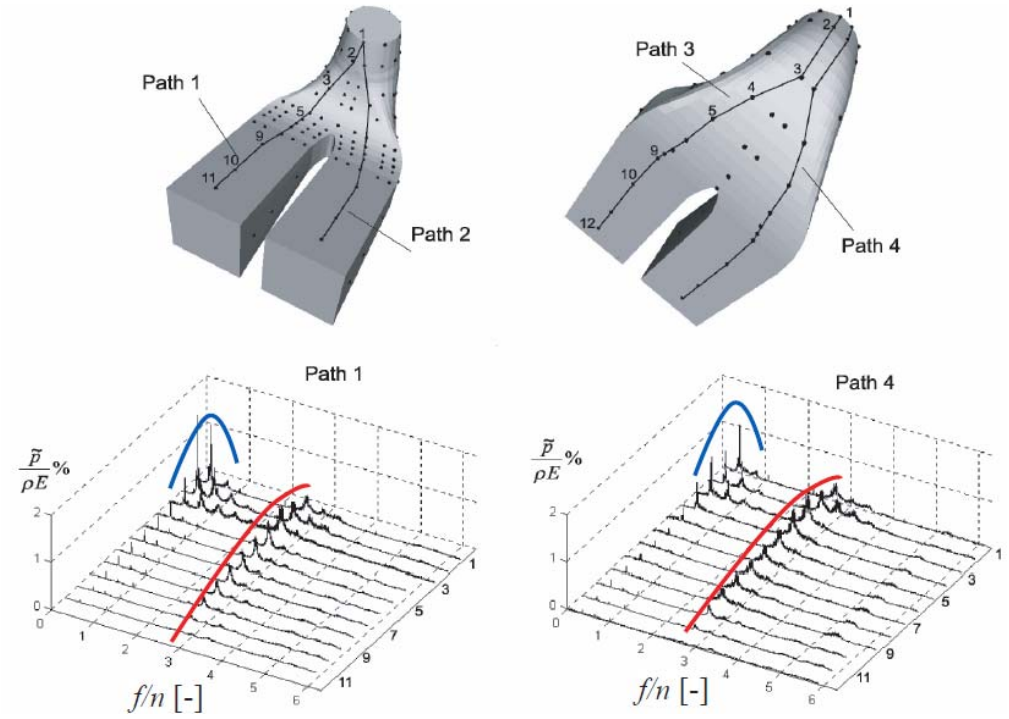

Fig. 3 Pressure fluctuations measured along the draft tube in case of upper part load resonance with the test rig, see [5]

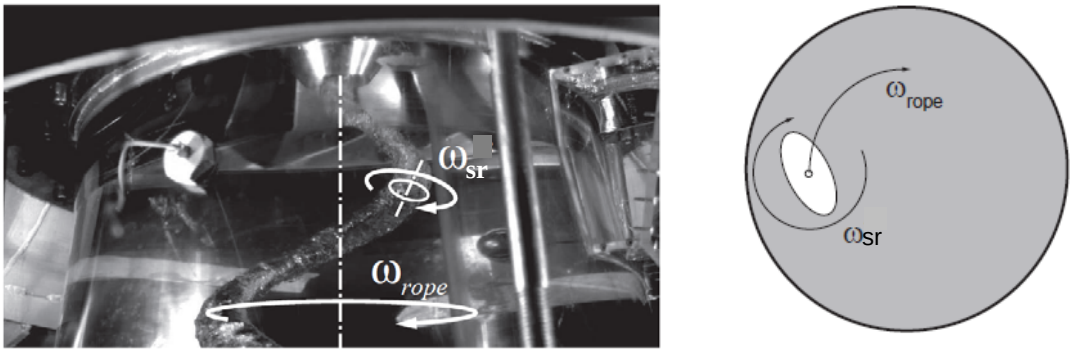

Fig. 4 Elliptical vortex rope precessing in the draft tube cone at upper part load

2. Case study and experimental apparatus

Pressure fluctuations measurements with synchronized draft tube vortex rope visualizations are carried out on a scale model Francis turbine with specific speed ν=0.5 installed in EPFL test rig, see

Fig. 5. The waterfall diagram of the pressure fluctuations in the draft tube cone are presented in

Fig. 1. The operating point featuring upper part load pressure fluctuation at rated discharge of 83% of the best efficiency point is selected for the experimental investigation and the related operating conditions are summarized in Table 1.

To perform the visualization of the vortex rope, a high speed camera Photron is used. The frame rate used for the investigation is 4000 frames/seconds using a diaphragm aperture time of 1/4000 s and a number of 3600 frames per movie. The images are obtained with a resolution of 1024×512 pixels. The lighting is ensured by 2 continuous spot lights of 600 W each located at 45°of each side of the high speed camera as shown in

Fig. 5. The Francis turbine scale model is equipped with 3 wall Quartz pressure transducers Kistler 701A measuring the unsteady part of the pressure. Two pressure transducers are located in the draft tube cone and the third one is located in the spiral case inlet, see

Fig. 5. The synchronization between the pressure acquisition and the image records is ensured by the trigger of an oscilloscope. The oscilloscope is used to store one second time history pressure signal with a sampling rate of 12.5 kHz. In parallel, the pressure is recorded using an HP 3566A PC Spectrum/Network Analyser system but without synchronization with the camera. These measurements are used for the representation of the waterfall diagram of the pressure fluctuations obtained by the averaging of 8 pressure amplitude spectra based on 4 seconds pressure time history with a sampling rate of 256 Hz.

Table 1 Parameter of the scale model Francis turbine and investigated operating point

Specific speed of the machine ν [-]	φ / φ_{BEP} [-]	ψ / ψ_{BEP} [-]	N [rpm]	GVO [°]
0.50	0.832	1.00	700	21.5

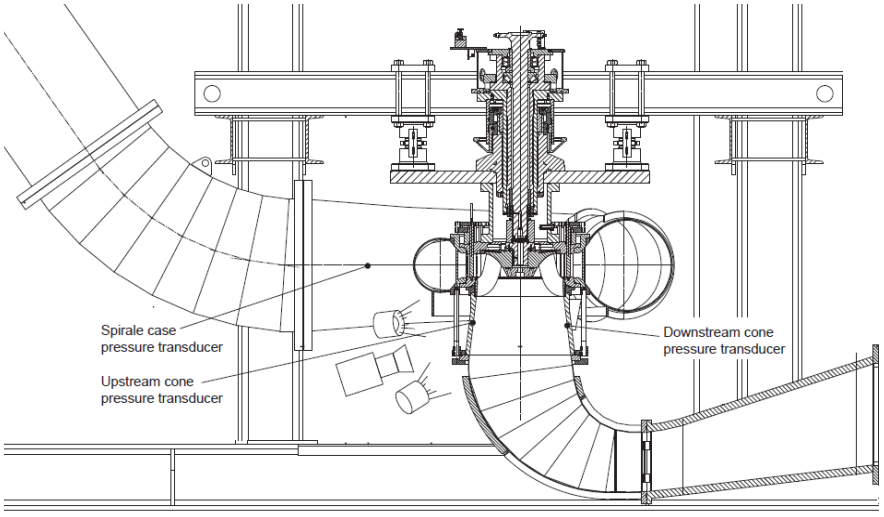

Fig. 5 Scale model installed on the EPFL test rig with high speed camera visualization

3. Influence of the cavitation number

The influence of the cavitation number σ, is analyzed for the operating point of Table 1 by considering 6 different cavitation numbers varying from σ = 0.1 to 0.3 and keeping the Froude number constant. The operating parameters as well as the observations are reported in the Table 2.

Table 2 Operating parameters for the influence of the cavitation number σ

N°	σ [-]	Froude Number [-]	N [rpm]	Observation
1	0.30	8.47	700	Hydroacoustic resonance, strong vortex rope shock on draft tube wall
2	0.26	8.47	700	Random hydroacoustic resonance, vortex rope shock on draft tube wall
3	0.22	8.47	700	
4	0.18	8.47	700	
5	0.14	8.47	700	Low outlet suction side bubble cavitation
6	0.10	8.47	700	Strong outlet suction side bubble cavitation

The pressure fluctuations measured at the upstream cone, downstream cone and spiral case for the 6 different operating points are presented in Fig. 6 as a waterfall diagrams. It can be noticed that the frequency of the pressure fluctuations in the range of 1 to 3 times the rotational speed increases with the cavitation number, similar to [4]. The frequencies and amplitudes related to the upper part load pressure fluctuations are reported in Fig. 7. The frequency increases almost linearly with the cavitation number while the amplitude of the pressure pulsations rises quickly up to 2.5% of the specific energy E for σ = 0.3. The amplitudes of pressure fluctuations for this cavitation number are similar for the 3 pressure transducers. In addition, strong mechanical vibrations and noise were noticed during the measurements. The shock phenomenon was also strongly present for these operating conditions. Thus, this operating point corresponds to the resonance between the vortex rope pressure fluctuations at f/n=~3 and the whole test rig.

Figure 8 left presents pictures of the vortex rope extracted from the movie synchronized with the pressure measurements represented on the top of the figure. This figure depicts the elliptical shape of the vortex rope self rotating at the pulsation ω_{sr} and precessing with a pulsation ω_{rope} for the resonance operating conditions, *i.e.* σ = 0.3. The five successive pictures extracted from the movie correspond to one period of the pressure fluctuations of interest T*; from $t = t_o$ to $t = t_o + T^*$. The influence of the pressure fluctuations on the dimensions of the vortex rope appears clearly, as for t = to, when the pressure is high, the vortex rope features small diameter while the diameter is the highest for t = to + T*/2 when the pressure is the lower. This pressure dependency is identical for the 6 operating points, see Nicolet [10]. Figure 8 right presents the same results for cavitation number σ = 0.22 where it can be noticed that, as expected, the mean diameter of the vortex rope increases as the cavitation number σ decreases. Moreover, the pressure fluctuations feature smaller amplitudes and a random like pattern. By analyzing the pictures of Fig. 8 it is found in agreement with Koutnik et al. [6], that the pulsation of the self rotation of the elliptical vortex rope ω_{sr} is half the pulsation of the measured pressure fluctuations ω*. Therefore, the combination between the rope precession ω_{rope} and the pressure fluctuations associated with the self rotation of the rope ω_{sr} illustrated in Fig. 4, leads to the modulation process already described by Arpe [11]. The elliptical shape of the vortex rope makes apparent the non-uniformity of the pressure distribution in the cross section of the cone which is portrayed in Fig. 9. Consequently, if the elliptical vortex rope rotates with the pulsation ω_{sr}, the associated pressure fluctuation features a pulsation of $\omega^* = 2 \cdot \omega_{sr}$.

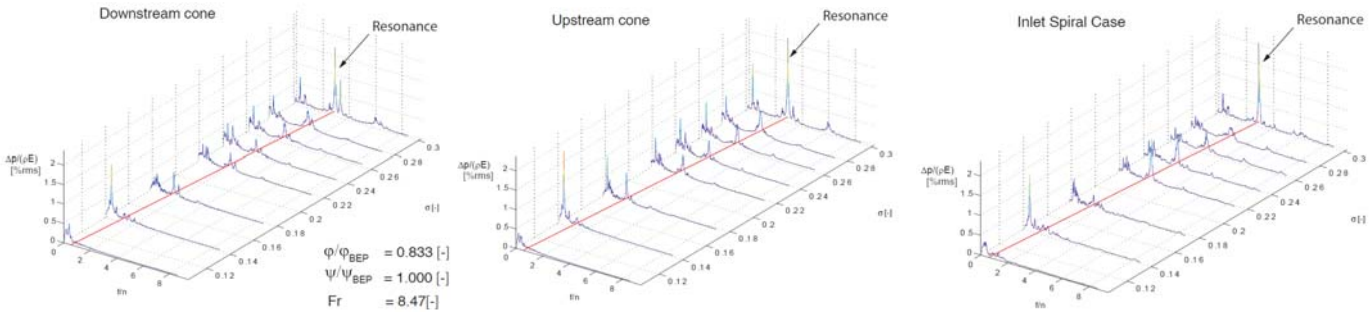

Fig. 6 Waterfall diagram of the pressure fluctuations measured at the downstream cone (left), upstream cone (center) and the spiral case (right) as function of the frequency and cavitation number

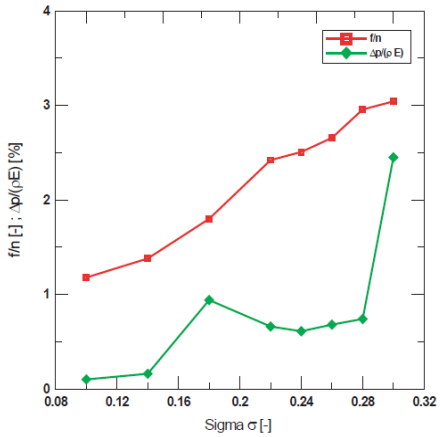

Fig. 7 Evolution of the frequency and amplitude of the pressure pulsations as function of the cavitation number at the downstream cone

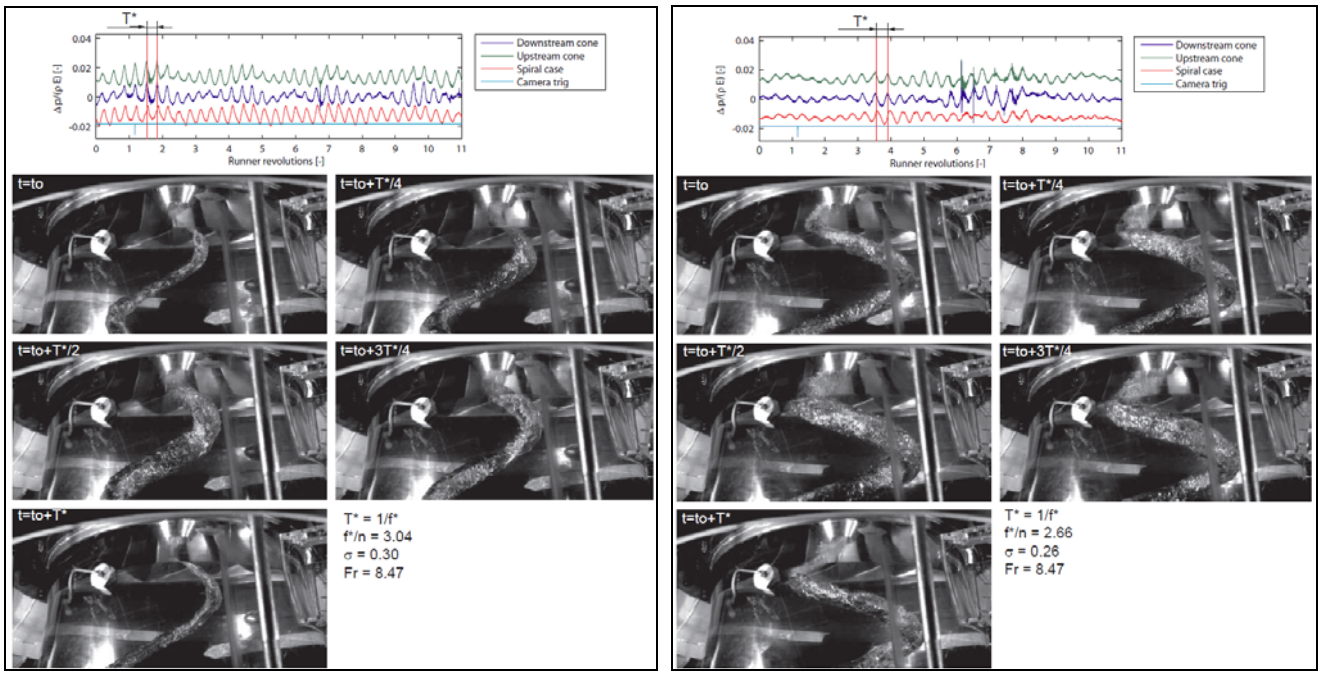

Fig. 8 Evolution of the vortex rope development for operating point N°1(left) and operating point N°2 (right), see Table 2

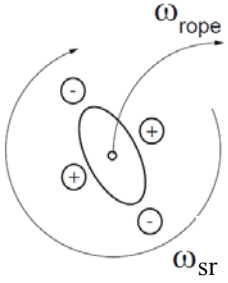

Fig. 9 Elliptical vortex rope with associated pressure distribution

4. Influence of outlet cavitation and air injection

Figure 10 presents the pictures of the vortex rope with the related synchronized pressure fluctuations for the operating points N°4 and N°5 obtained respectively with cavitation number σ=0.18 and σ=0.14, see Table 2. It can be noticed that the reduction of the cavitation number from σ=0.18 to σ=0.14 induces outlet bubble cavitation on the suction side evidenced at t=to+T*/2 of operating point N°5, see

Fig. **10** right. This cavitation also induces additional high frequency pressure fluctuations visible on the downstream and upstream cone pressure time history. Moreover, the appearance of outlet bubble cavitation induces a strong reduction of pressure fluctuation amplitudes associated with the vortex rope self rotation as it is illustrated in Fig. 7 with an amplitude reduction from 1% to 0.2% of the specific energy E. To confirm the effect of outlet bubble cavitation on the pressure fluctuations associated with the vortex rope self rotation, air was injected at the turbine for the operating point N°4. The resulting effect on cavitation and pressure pattern is visible in Fig. 11 and can be compared with the results presented without air injection in

Fig. **10** left. The increase of the cavitation nuclei content in the bulk flow originating from the upstream air injection promotes runner outlet bubble cavitation. Then, a strong decrease of the pressure fluctuation at the vortex rope self-rotation is observed while high frequency pressure fluctuations due to the bubble cavities appear. With air injection, the frequency of these pressure fluctuations is also decreasing to a value close to the value obtained when the cavitation number is reduced to σ=0.14. The positive effect of air injection was also reported by Koutnik *et al.*, see [8]. This positive effect may be either attributed to (i) a modification of the hydraulic system natural frequencies due to a higher cavitation volume or air content, and thus leads to a mistuning with the excitation source frequency, or (ii) to a draft tube flow distortion induced by the outlet bubble cavitation affecting the excitation mechanism.

With respect to the second hypothesis, on prototype, it is expected to have more developed outlet bubble cavitation than on the model due to higher air content and to higher head, see Henry *et al.* [12] and Gindroz *et al*. [13]. Therefore, it could be suspected that the prototype features outlet bubble cavitation which is not present on model tests that would help mitigating the upper part load pressure fluctuations in the range from 1 to 3 times the rotational speed. This hypothesis is also well correlated with the fact that Fischer *et al.* [1] and Koutnik *et al.*, see [8] are mentioning that the upper part load pressure fluctuations problems were not reported on prototype so far. Since then, upper part load pressure fluctuations have been reported on prototype and fixed by using another runner design, *i.e.* another draft tube flow, see Shi [14]. However, more investigations would be required to clearly understand the positive effect of air injection.

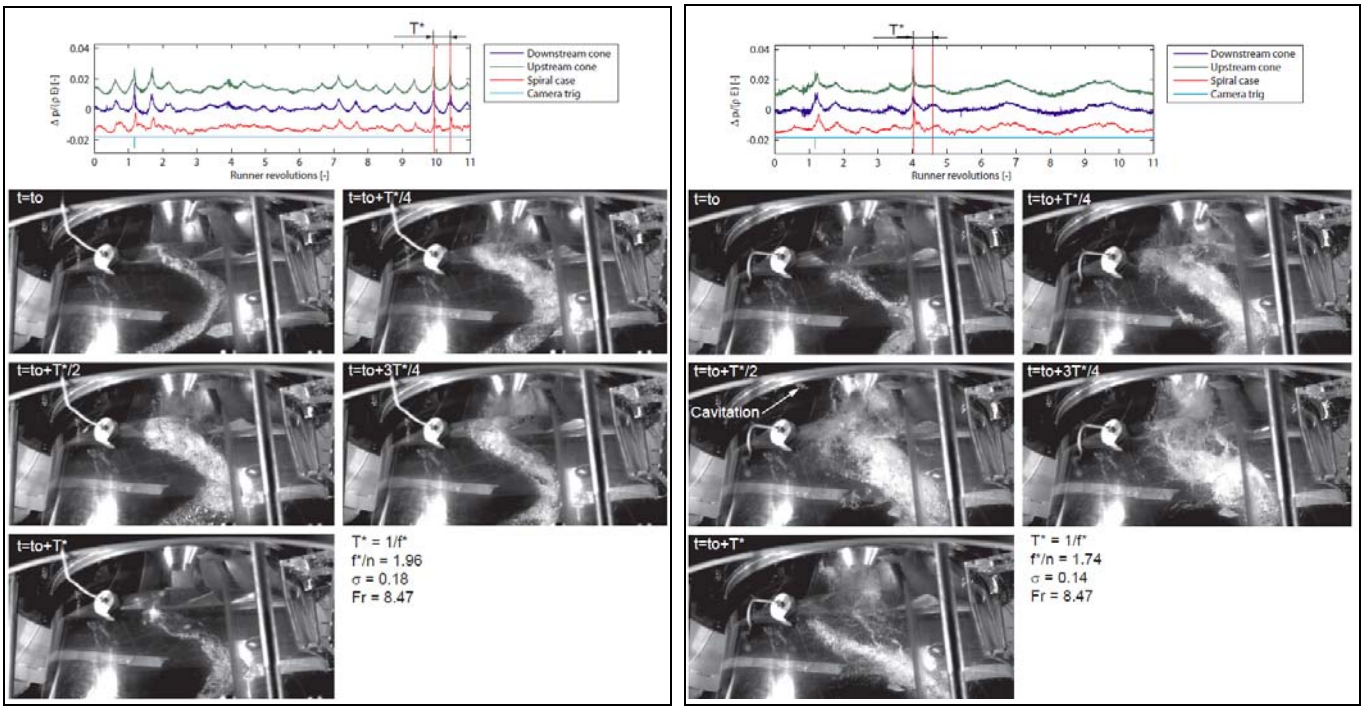

Fig. 10 Evolution of the vortex rope development for operating point N°4(left) and operating point N°5 (right), see Table 2

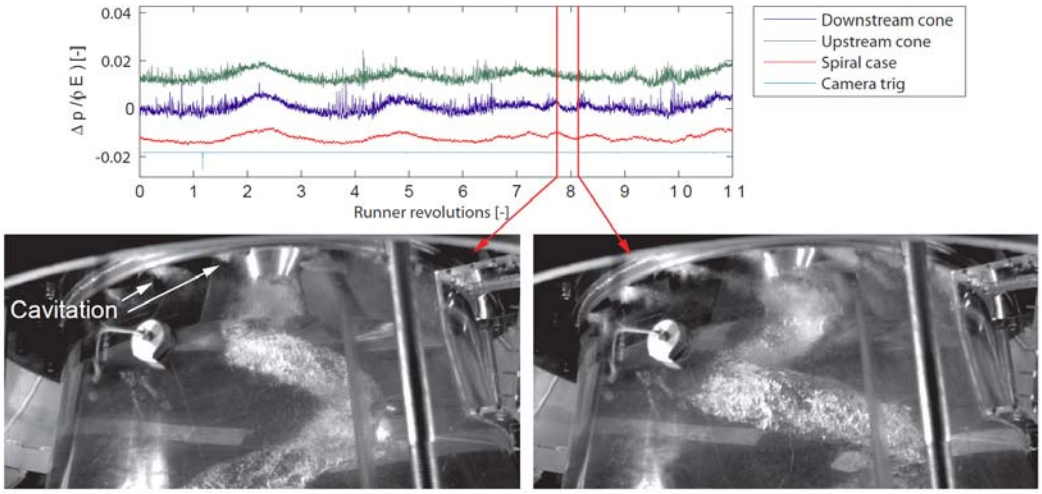

Fig. 11 Vortex rope development for operating point N°4 with air injection, σ=0.18 and Fr=8.47, see Table 2

Moreover, the complex flow structure at the runner outlet is evidenced by the modification of the cavitation development during pressure variations obtained for the operating point N°5, see
Fig. **10** right. Figure 12 presents a schematic view of the cavitation structure at the runner outlet featuring small cavitating vortices attached to the runner cone and rotating on themselves at the pulsation ω_2, while the vortex rope self-rotation at the pulsation ω_{sr} appears to be made of two vortex ropes animated with a self-rotation ω_1.

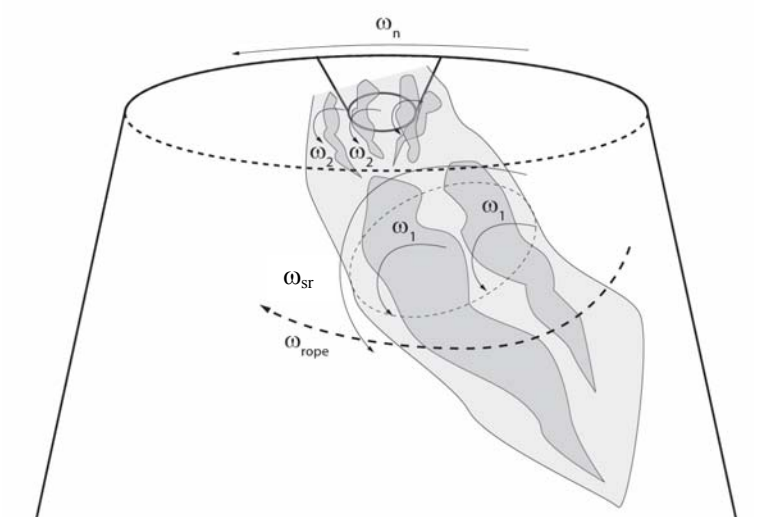

Fig. 12 Vortex rope structure for the operating point N°5 with σ=0.14 and Fr=8.47, see Table 2

5. Vortex rope volume time evolution

The influence of the pressure fluctuations on the vortex rope volume is analyzed by post processing the images of the movie related to operating point N°1 with σ = 0.3. The post processing methodology is described in

Fig. 13. First, a part of the image focusing on the vortex rope is extracted. Then, the image is filtered in order to obtain black and white image of the vortex rope. The black area of the image A_b and the white area of the image A_w are computed in terms of pixels enabling to compute the ratio of white area as $A_w/(A_w+A_b)$. This ratio is representative of the vortex rope diameter. This image processing is carried out for all the 3600 images of the movie of operating point N°1 with σ = 0.3 and are presented as function of time in Fig. 14 left. The pressure fluctuation time history is presented in this figure and synchronized in time with the time evolution of the vortex rope volume using the camera start trig. It can be noticed that, as identified from Fig. 8, the volume of the vortex rope is always maximum when the pressure is minimum and *vice versa*. The period of the pressure fluctuations T* and the period of the vortex rope precession T_{rope} can be clearly identified. Moreover, the ratio of white area calculated from image processing is represented as a function of the pressure in the draft tube and in spiral case for one period of pressure fluctuation T* in Fig. 14 right. It can be noticed that the curves related to the pressure in the cone feature breathing like pattern and describe surfaces counter-clockwise indicating that the vortex rope is providing energy to the hydraulic system and behaves as an energy source, [6]. Similar self excitation pattern can be found in case of full load operation where the diffuser effect of the draft tube geometry has been found to play a strong role, see [15].

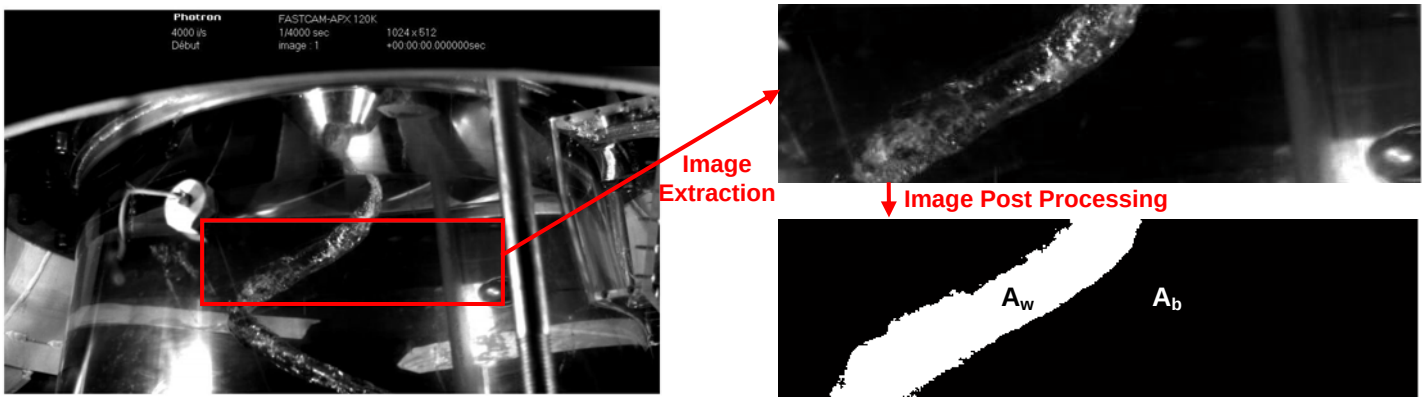

Fig. 13 Image post processing for vortex rope volume time history determination

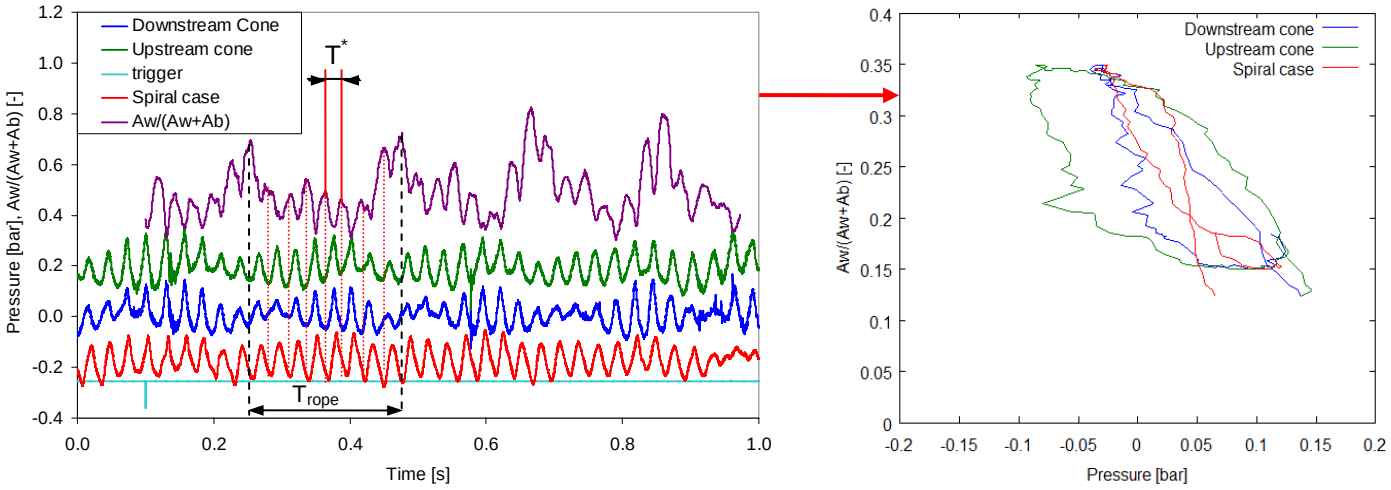

Fig. 14 Time evolution of the vortex rope area and synchronized pressure fluctuations (left) and vortex rope area *versus* pressure (right)

6. Influence of the Froude number

The operating conditions chosen for the investigation of the influence of the Froude number are identical as the previous operating point in terms of discharge coefficient and specific energy coefficient given in Table 1, but the cavitation number is kept constant and equal to σ = 0.30 in order to focus on the conditions of resonance of the test rig. The Froude number is given by $Fr = C_{ref} / \sqrt{g \cdot L_{ref}}$ which can be expressed, considering the reference velocity as $C_{ref} = \sqrt{E}$ as follows:

$$Fr = \sqrt{H / L_{ref}} \tag{1}$$

The Froude number affects the distribution of cavitation in the flow as it determines the pressure gradient relatively to the size of the machine. The relation between the position of the vapor pressure p_v can be expressed as a function of the Froude number, see Franc *et al.* [16], neglecting Reynolds effects, assuming the same cavitation number σ as a function of the reference position Z_{ref} as follows:

$$\frac{Z_{ref} - Z_1}{Z_{ref} - Z_2} = \frac{Fr_1^2}{Fr_2^2} \tag{2}$$

The Froude number being usually smaller on prototype than in the model, the elevation of the position of the cavitation is higher on prototype than in the model, [16], and [17]. Due to the difference of Froude numbers, the vortex rope on scale model is more narrow and longer than on prototype as illustrated in Fig. 15, see Dörfler [18].

For these investigations, four different values of the Froude number are taken into account and are obtained by varying the rotational speed of the turbine. The operating conditions considered for this investigation are presented in the Table 3. The wall pressure fluctuations measured at the downstream cone, upstream cone and spiral case are presented as function of the frequency and Froude number in Fig. 16 as waterfall diagram.

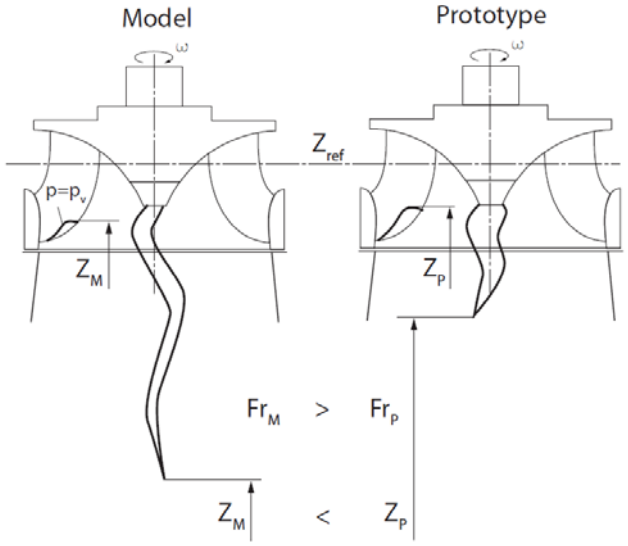

Fig. 15 Difference of the cavitation development between model (M) and prototype (P) due to difference in Froude numbers

Table 3 Operating conditions for the influence of the Froude number

N°	σ [-]	Froude Number [-]	N [rpm]	Remark
1	0.30	8.47	700	Hydroacoustic resonance, and mechanical vibrations
7	0.30	7.86	650	Hydroacoustic resonance, and mechanical vibrations
8	0.30	7.26	600	Low hydroacoustic resonance, and mechanical vibrations
9	0.30	6.64	550	Low hydroacoustic resonance, and mechanical vibrations

First, it can be noticed from the observations of Table 3 that hydroacoustic resonance and mechanical vibrations are observed for all tested conditions, even if the level of resonance and related vibration were lower for lower values of the Froude number. This is partly due to the fact that decreasing the Froude number leads to a reduction of the specific energy and therefore of the absolute magnitude of the pressure fluctuations. However, as it is reported by the waterfall diagram of Fig. 16, the relative amplitudes of pressure fluctuations is also reducing when the Froude number is decreasing. Figure 17 represents the amplitude and frequency of the pressure pulsations of interest as function of the Froude number. It can be noticed that the frequency of the pressure pulsations are proportional to the runner rotational speed, in accordance with Koutnik *et al.* [8], and that the amplitudes are of the same order of magnitude for the values of Froude equal to Fr = 8.47 and 7.86, while they are divided at least by a factor 2 for Fr = 7.26 and 6.64. The reason is that the resonance phenomenon features more random behaviour for Fr = 7.26 and 6.64 than for Fr = 8.47 and 7.86, as it is illustrated in Fig. 18.

No visualizations of the vortex rope are presented here as the shape of the vortex rope was not very much affected by the Froude number, at least in the range of tested Froude values, and therefore does not affect significantly the wave speed in the draft tube. It means that the eigen frequencies of the test rig, including the turbine and the draft tube, are not strongly affected by the change of the Froude number in the tested range. Then changing the rotational speed of the runner results in a mistuning between the excitation source, illustrated by the vortex rope self-rotation, with associated pressure pulsation ω*, and the eigen frequency of the full hydraulic system. It results in a situation where there is no more strict resonance but random resonance. This means that the observed

phenomenon is really of the resonance type. Similar conclusions have been found by Koutnik *et al.* [6] who found also a small part of self-excitation observing the pressure *versus* rope volume dependence.

The modulation process between the vortex rope precession and the pressure associated with self-rotation of the vortex rope, f_{rope} and f^* respectively, is illustrated by the amplitude spectra measured for Fr = 7.86. Therefore, the time plots and related amplitude spectra are represented in Fig. 19 where it can be clearly seen that modulation between the two dominant pulsations leads to amplitudes in the spectrum for $f = f^* \pm f_{rope}$, $f^* \pm 2 \cdot f_{rope}$, $f^* \pm 3 \cdot f_{rope}$, *etc* and for $f = 2 \cdot f^* \pm f_{rope}$, $f^* \pm 2 \cdot f_{rope}$, $f^* \pm 3 \cdot f_{rope}$, *etc*. It can be noticed that in this case, the self rotation of the vortex rope does not corresponds to a multiple of the vortex rope precession frequency: $f^* = 7.5 \cdot f_{rope}$.

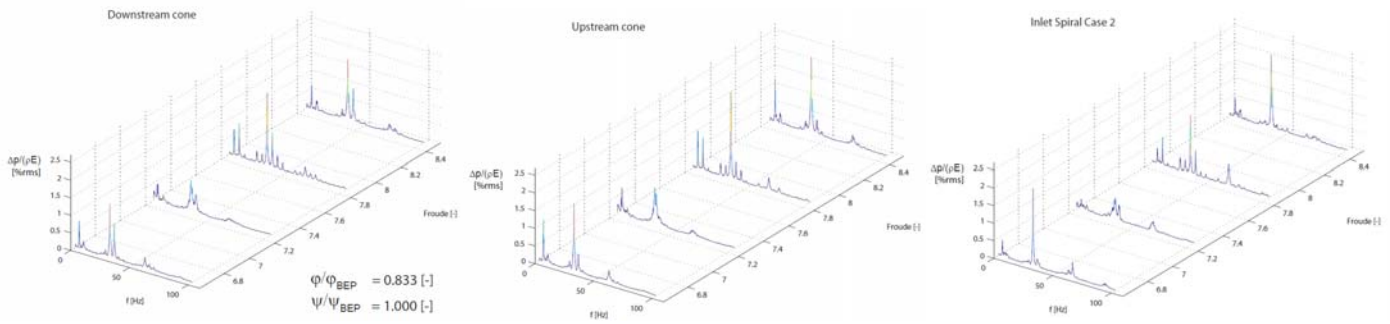

Fig. 16 Waterfall diagram of the pressure fluctuations at the downstream cone (left), upstream cone (center) and the spiral case (right) as function of the frequency and Froude number for σ = 0.3

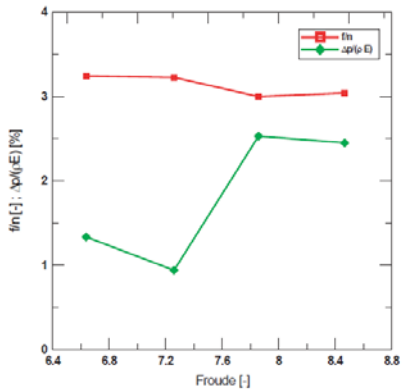

Fig. 17 Evolution of the frequency and amplitude of the pressure pulsations as function of the Froude number at the downstream cone for σ = 0

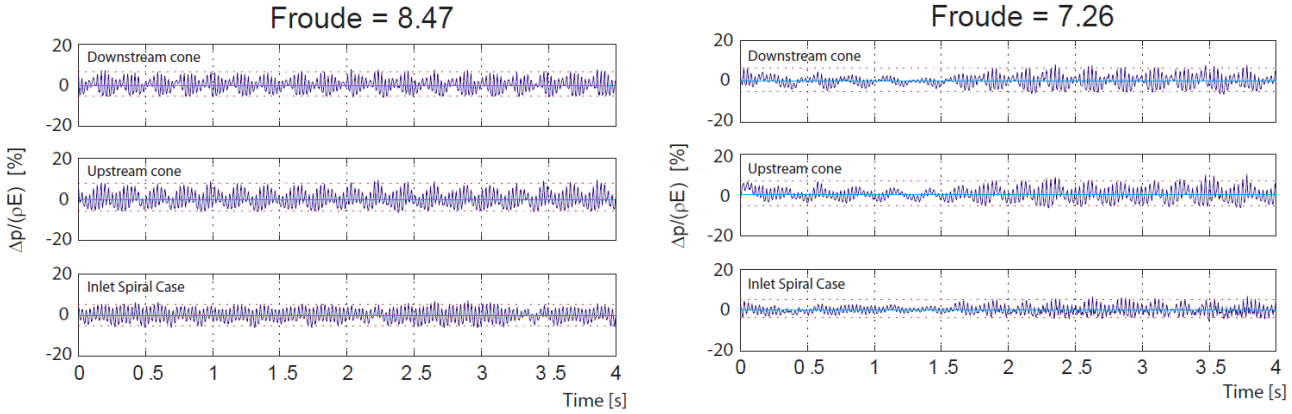

Fig. 18 Pressure fluctuations time history obtained in downstream cone, upstream cone and spiral case for σ=0.3 with Fr=8.47 (left) and Fr=7.26 (right)

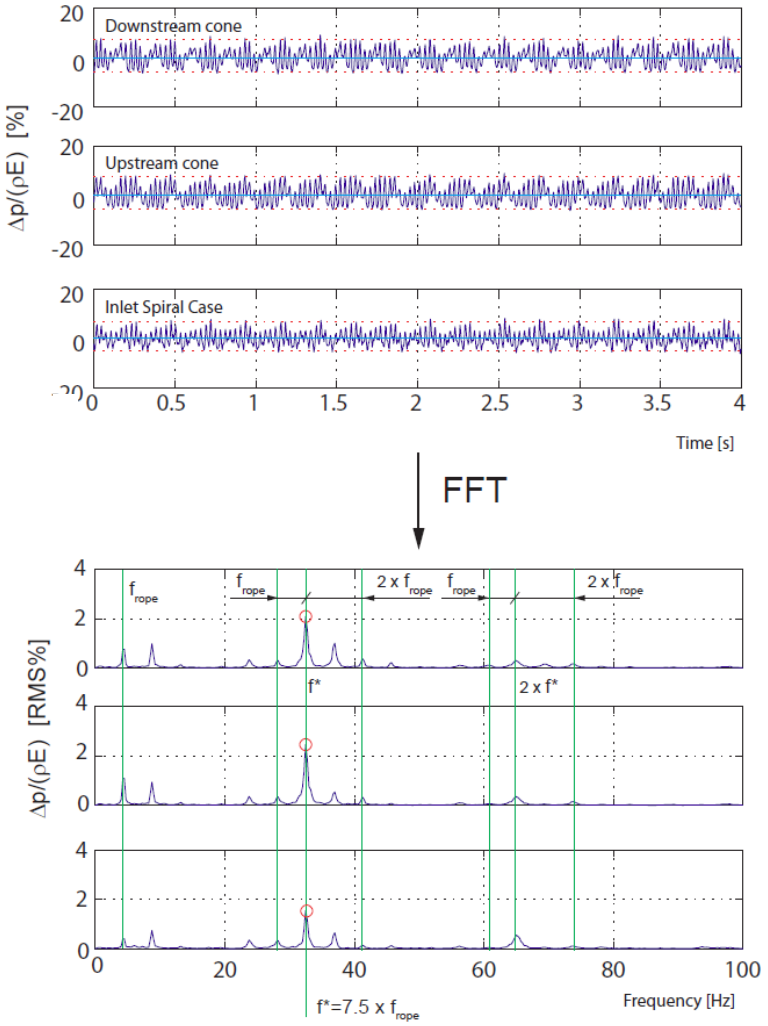

Fig. 19 Modulation of the pressure pulsation at the vortex rope precession frequency f_{rope} and pressure pulsation f^* for σ = 0.3 and Froude =7.86

7. Conclusion

An experimental investigation on a reduced scale Francis turbine of specific speed ν = 0.5 was performed using wall pressure measurements synchronized with movie recording. The upper part load is characterized by pressure pulsations in the range of f/n = 1 to 3. The flow visualizations with simultaneous pressure measurements show that the vortex rope features an elliptical cross section and that the vortex rope is self rotating at a frequency half of pressure fluctuations of interest. This particular structure of the flow leads to modulation of the pressure fluctuations related to the vortex rope precession and of the pressure fluctuations of interest.

For low cavitation number, it has been found that the amplitudes of the pressure fluctuations in the range f/n = 1 to 3 reduces drastically when outlet bubble cavitation develops. The same positive effect can be obtained by upstream air injection that reveals outlet bubble cavitation for a higher cavitation number.

Image processing enabled to point out that the vortex volume is changing according to pressure and features breathing like pattern and behaves as an excitation source. The pressure fluctuations appear to be strongly linked to the cavitation number and therefore resonance conditions are commonly encountered during model tests when the excitation source of the vortex rope in the range of f/n = 1 to 3 matches the hydraulic system eigen frequencies. The Froude investigation shows that the pressure fluctuation frequency is proportional to the rotational speed, and therefore the draft tube flow behaves as an excitation source but with excitation frequencies above the rotational speed.

As shown in this paper, the upper part load pressure fluctuations is a complex phenomenon that will require more experimental and numerical investigations to be understood as it features different aspects such as vortex rope precession, vortex rope self rotation, pressure fluctuations modulation process, shock phenomenon, interaction with the hydraulic system and possible resonance and breathing like pattern pointing out energy source pattern.

Acknowledgments

The authors would like to thank Etienne Vuadens, Ambrosio Acal Ganaza and Philippe Ausoni from LMH for their help in the setup of the acquisition system and signal post processing. The authors also would like to thank all the staff from the model testing group of the EPFL Laboratory for Hydraulic Machines for their support for the set up of the experimental facilities.

Nomenclature

A	Image area, pixels	n	Runner rotational frequency, Hz
C	Absolute mean flow speed, m/s, $C = Q/A$	p	Pressure, Pa.
E	Machine specific energy, J/kg, $E = gH_1 - gH_2$	p_v	Vapor pressure, Pa
Fr	Froude number,	g	Gravity acceleration, m/s^2
H	Head, m	ρ	Water density, kg/m^3
L_{ref}	Reference length, m	φ	Discharge coefficient, $\varphi = Q/\pi\omega R_{ref}^3$
N	Rotational speed, rpm	ψ	Specific energy coefficient, $\psi = 2E/\omega^2 R_{ref}^2$
Q	Flow rate, m^3/s, $Q = C \cdot A$	ν	Machine specific speed, $\nu = \varphi^{1/2}/\psi^{3/4}$
R_{ref}	Machine reference radius, m	ω	Pulsation, rad/s
T	Period, s	ω_{rope}	Pulsation of the vortex rope precession, rad/s
Z	Elevation, m		
f	Frequency, Hz, $f = 1/T$	ω^*	Pulsation of vortex rope self rotation pressure fluctuations, rad/s
f_{rope}	Frequency of the vortex rope precession, Hz		
f^*	Frequency of the vortex rope self rotation pressure fluctuations, Hz	σ	Cavitation number, $\sigma = (p_{ref} - p_v)/1/2\rho C_{ref}{}^2$
		BEP	Best efficiency point

References

[1] Fisher, R. K., Palde, U., Ulith, P., 1980, "Comparison of draft tube surging of homologous scale models and prototype Francis turbines," In Proceeding of the 10th IAHR Symposium on Hydraulic Machinery and Systems (Tokyo, 1980), pp. 541-556.

[2] Dörfler, P. K., 1994, "Observation of the pressure pulsation on Francis model turbine with high specific speed," Hydropower & Dams (January 1994), 21-26.

[3] Jacob, T., and Prenat, J.-E., 1996, "Francis turbine surge : discussion and database," In Proceeding of the 18th IAHR Symposium on Hydraulic Machinery and Systems (Valencia, Spain, 1996), vol. 2, pp. 855-864.

[4] Nicolet, C., Arpe, J. And Avellan, F., 2004, "Identification and modeling of pressure fluctuations of a Francis turbine scale model at part load operation," Proceedings of the 22nd IAHR Symposium on Hydraulic Machinery and Systems, Stockholm, Sweden, June 29 - July 2, 2004.

[5] Arpe, J., Nicolet, C., Avellan, F., 2009, "Experimental Evidence of Hydroacoustic Pressure Waves in a Francis Turbine Elbow Draft Tube for Low Discharge Conditions," ASME, J. Fluids Eng., Volume 131, Issue 8, August 2009.

[6] Koutnik, J., Krüger, K., Pochyly, F., Rudolf, P., and Haban, V., 2006, "On cavitating vortex rope form stability during Francis turbine part load operation," In Proceedings of the first Meeting of the IAHR Int. Working Group on Cavitation and Dynamic Problems in Hydraulic Machinery and Systems (Barcelona, June 2006).

[7] Habán, V., Rudolf, P., Pochylý, F., Koutník, J., Krüger, K., 2007, "Stability of infinitely long asymmetrical vortex rope", Proceedings of the 2nd IAHR International Meeting of the WorkGroup on Cavitation and Dynamic Problems in Hydraulic Machinery and Systems, Timisoara, Romania, October 24-26, 2009.

[8] Koutnik, J., Faigle, P., Moser, W., 2008, "Pressure fluctuations in Francis turbines - theoretical prediction and impact on turbine," Proceedings of the 24th IAHR Symposium on Hydraulic Machinery and Systems, Foz do Iguassu, Brazil, October 27-31, 2008, paper 118.

[9] Kirschner, O., Ruprecht, A., Göde, E., 2009, "Experimental investigation of pressure pulsation in a simplified draft tube," Proceedings of the 3rd IAHR International Meeting of the WorkGroup on Cavitation and Dynamic Problems in Hydraulic Machinery and Systems, Brno, Czech Republic, October 14-16, 2009, paper B1, pp. 55-64.

[10] Nicolet, C., 2007, "Hydroacoustic Modelling and Numerical Simulation of Unsteady Operation of Hydroelectric Systems," PhD Thesis, EPFL n°3751, Lausanne, (http://library.epfl.ch/theses/?nr=3751).

[11] Arpe, J., 2003, "Analyse du champ de pression pariétale d'un diffuseur coudé de turbine Francis," PhD Thesis, EPFL n°2779, Lausanne.

[12] Henry, P., Lecoffre, Y., Larroze, P. Y., "Effets d'echelle en cavitation," Proceedings of 10th IAHR Symposium on Hydraulic Machinery and Systems, Tokyo, Japan, pp. 103-114.

[13] Gindroz B., Avellan F., Henry P.; "Guidelines for performing cavitation tests", Proceedings of the 15th IAHR Symposium on Hydraulic Machinery and Cavitation, 11-14 September 1990, Belgrade, Yugoslavia, Vol. I, paper H1.

[14] Shi, Q., 2010 "Hydraulic design of Three Gorges right bank powerhouse turbine for improvement of hydraulic stability," Proceedings of the 25th IAHR Symposium on Hydraulic Machinery and Systems, Timisoara, Romania, September 20-24, 2010, paper 1A.1

[15] Chen, C., Nicolet, C., Yonezawa, K., Farhat, M., Avellan, F., Miyagawa, K.,, Tsujimoto, Y., "Experimental Study and Numerical Simulation of Cavity Oscillation in a Conical Diffuser," International Journal of Fluid Machinery and Systems, Vol. 3, No. 1, January-March 2010, pp. 91-101.

[16] Franc, J.-P., Avellan, F., Belhadji, B., Billard, J.-Y., Brianc¸ Marjolet, L., Fréchou, D., Fruman, D. H., Karimi, A., Kueny, J.-L., Michel, J.-M. 1995, "La Cavitation: Mécanismes Physiques et Aspects Industriels," Collection Grenoble Sciences. Presse Universitaires de Grenoble, Grenoble, (in french).

[17] Jacob, T. 1994, "Similitude in stability of operation tests for Francis turbine," Hydropower & Dams, Volume I, January.

[18] Dörfler, P. K., 1982, "System oscillations excited by the Francis turbine's part load vortex core: mathematical modeling and experimental verification," PhD thesis, Techn. University Vienna, Vienna, (in german).